Synthesis of In-House Produced Calibrated Silver Phosphate with a Large Range of Oxygen Isotope Compositions

Christophe Lécuyer, François Fourel, Magali Seris, Romain Amiot, Jean Goedert, Laurent Simon

Synthesis of In-House Made Calibrated Silver Phosphate in a Large Range of Oxygen Isotope Compositions

Christophe **Lécuyer**[1,*], François **Fourel**[2], Magali **Seris**[1], Romain **Amiot**[1], Jean **Goedert**[1,3] and Laurent **Simon**[2]

[1]LGL-TPE, UMR 5276, CNRS, Université Claude Bernard Lyon 1, 69622 Villeurbanne, France

[2]LEHNA, UMR 5023, CNRS, Université Claude Bernard Lyon 1, ENTPE, 69622 Villeurbanne, France

[3]PACEA, UMR 5199, CNRS, Université de Bordeaux, Bâtiment B18, Allée Geoffroy Saint-Hilaire, CS 50023, FR-33615 Pessac, France

*corresponding author. E-mail : christophe.lecuyer@univ-lyon1.fr

Abstract – The large range of stable oxygen isotope values of phosphate-bearing minerals and dissolved phosphate of inorganic or organic origin requires the availability of in-house made calibrated silver phosphate of which isotopic ratios must closely bracket those of studied samples. We propose a simple protocol to synthesize Ag_3PO_4 in a wide range of oxygen isotope compositions based on the equilibrium isotopic fractionation factor and the kinetics and temperature of isotopic exchange in the phosphate-water system. Ag_3PO_4 crystals are obtained from KH_2PO_4 that is dissolved in water of known oxygen isotope composition. Isotopic exchange between dissolved phosphate and water takes place at a desired and constant temperature into pyrex tubes that are placed in a high precision oven for run-times defined by the user. Samples are withdrawn at desired times, quenched in cold water, and precipitated as Ag_3PO_4. We provide a calculation sheet that computes the $\delta^{18}O$ of precipitated Ag_3PO_4 as a function of time, temperature and $\delta^{18}O$ of both reactants KH_2PO_4 and H_2O at t = 0. Predicted oxygen isotope compositions of synthesized silver phosphate range from -7 to +31‰ VSMOW for a temperature range comprised between 110°C and 130°C and a range of water $\delta^{18}O$ from -20 to +15‰ VSMOW.

Keywords: oxygen isotopes, isotopic fractionation, kinetics, silver phosphate, internal reference

Résumé – La large gamme de $\delta^{18}O$ des minéraux phosphatés et de phosphates dissous d'origine inorganique ou organique nécessite l'existence d'Ag_3PO_4 calibré dont les rapports isotopiques doivent encadrer les échantillons étudiés. Nous proposons un protocole simple pour synthétiser Ag_3PO_4 dans une large gamme de compositions isotopiques. Ce protocole repose sur les fractionnements isotopiques à l'équilibre et les températures et cinétiques d'échange isotopique dans le système phosphate-eau. Les cristaux d'Ag_3PO_4 sont obtenus à partir de KH_2PO_4 dissous dans une eau de $\delta^{18}O$ connu. Les échanges isotopiques entre le phosphate dissous et l'eau ont lieu à une température constante dans des tubes en pyrex placés dans une étuve thermo-régulée pour des durées de réactions définies par l'opérateur. Les échantillons sont retirés en temps voulu, trempés dans de l'eau froide, et précipités sous la forme de cristaux de phosphate d'argent. Nous fournissons une « feuille Excel » qui calcule le $\delta^{18}O$ d'Ag_3PO_4 précipité en fonction du temps, de la température et des $\delta^{18}O$ de KH_2PO_4 et H_2O au temps t = 0. Les $\delta^{18}O$ prédits pour Ag_3PO_4 varient de -7 à +31‰ VSMOW pour une gamme de températures comprises entre 110°C et 130°C et une gamme de $\delta^{18}O$ de l'eau de -20 to +15‰ VSMOW.

Mots-clés: isotopes de l'oxygène, fractionnement isotopique, cinétique, phosphate d'argent, référence interne

1. Introduction

During the past decades, the rise of automated devices coupled to mass spectrometers operating in continuous flow or in dual-inlet mode resulted in an explosive growth of the

63 number of data published in the scientific fields exploiting the stable isotope ratios of organic
64 and inorganic compounds. Consequently, there is an increasing use and need for developing in-
65 house made material calibrated against certified reference materials. Moreover, a large range
66 of isotopic compositions is highly desirable to bracket the expected compositions of the studied
67 sample collection as well as to be able to perform a two-point calibration, which is required for
68 the acquisition of high-quality data.

69 In Earth and Archaeological Sciences, to only mention the most concerned research
70 fields, the $^{18}O/^{16}O$ ratio of the phosphate radical (PO_4^{3-}) is now widely used to reconstruct the
71 paleoclimates of the Earth (Fricke and O'Neil, 1996; Kolodny and Raab, 1988; Amiot et al.,
72 2004; Joachimski et al., 2012; Goedert et al., 2017), the thermophysiology and ecology of
73 extinct vertebrates (Barrick and Showers, 1994; Fricke and Rogers, 2000; Amiot et al., 2006;
74 Tütken and Vennemann, 2009; Bernard et al., 2010; Rey et al., 2018), the source and recycling
75 of dissolved phosphate in natural waters (Markel et al., 1994; McLaughlin et al., 2006; Pistocchi
76 et al., 2017) as well as the diet and living environment of past human populations (White et al.,
77 1998; Evans and Chenery, 2006; Touzeau et al., 2013; Lightfoot and O'Connell, 2016;
78 Pellegrini et al., 2016). The most common way to determine the $^{18}O/^{16}O$ ratio of the phosphate
79 radical is to isolate it as silver phosphate (Ag_3PO_4) crystals through a wet chemistry procedure
80 (Crowson et al., 1991). Then they are pyrolyzed in the presence of graphite at high temperature
81 to produce either CO_2 or CO analysed either off-line or on-line with an isotopic ratio mass
82 spectrometer (O'Neil et al., 1994; Lécuyer et al., 1998; 2007; Fourel et al., 2011). Fluorination
83 technique has also been proven to be a precise and accurate technique that allowed the first
84 determination of the $\delta^{18}O_{SMOW}$ of the Miocene Florida phosphorite SRM 120c (Lécuyer et al.,
85 1993). Whatever the considered research field, the $\delta^{18}O$ of calcium phosphate minerals (e.g.

86 biogenic, magmatic or hydrothermal apatite) and dissolved phosphate ($H_2PO_4^-$, HPO_4^{2-}, PO_4^{3-}
87) range worldwide from about a few per mil up to values close to 30‰. Indeed, high-
88 temperature apatites of magmatic or hydrothermal origin have $\delta^{18}O$ ranging from 6 to 11‰
89 Sun et al., 2016). Concerning soils and their connected aquatic environments (rivers, ponds,
90 lakes), dissolved phosphate also displays a large range of oxygen isotope compositions
91 comprised between 8‰ and 25‰ (Markel et al., 1994; Gruau et al., 2005; Angert et al., 2012;
92 Davies et al., 2014; Tamburini et al., 2014; Pistocchi et al., 2017; Granger et al., 2017; Bauke
93 et al., 2018). In the case of dissolved phosphate being isotopically equilibrated with ambient
94 water through biological recycling (Longinelli et al., 1976; Liang and Blake, 2009; Chang and
95 Blake, 2015; von Sperber et al., 2017), it is expected to have $\delta^{18}O$ that range from 6‰ (high-
96 latitude freshwater environments) to ≈ 20‰ for seawater and to ≈ 22‰ for low-latitude
97 freshwater environments in agreement with the available isotopic fractionation equations
98 (Kolodny et al., 1983; Lécuyer et al., 2013). In the case of biogenic apatites, their $\delta^{18}O$ values
99 range from a few ‰ for vertebrates drinking highly ^{18}O-depleted waters ($\delta^{18}O$ as low as -20‰)
100 relative to SMOW (high-altitude or high-latitude environments; e.g. Rey et al., 2018) up to
101 about 30‰ for vertebrates living in arid environments (Lécuyer et al., 1999a).

102 So far, researchers were using the Florida phosphorite SRM 120c, for which a
103 consensual $\delta^{18}O_{SMOW}$ value of 21.7±0.2‰ (VSMOW) was only admitted these last years.
104 Indeed, Chenery et al. (2010) proposed a comparable value of 21.7±0.7‰ after a 6-month
105 period of repeated measurements of SRM 120c calibrated against NBS 127 barium sulfate,
106 which is consistent with the average value of published data for SRM 120c (21.5±0.5‰)
107 analyzed in different laboratories (Chenery et al., 2010). Thereafter, Halas et al. (2011)
108 confirmed the absence of any sizable isotopic fractionation effect during the conversion of

Ag_3PO_4 into CO, and proposed a mean $\delta^{18}O$ value of 21.8±0.2‰ for SRM 120c based on inter–laboratory calibrations. It is also worthy to note that Vennemann et al. (2002) proposed a significantly higher value of 22.5‰ for SRM 120c. But later on, in a communication given at 'IsoPhos' meeting in Ascona, Switzerland, Vennemann (2012) concluded that the most accurate value for SRM 120c is likely close to 21.7‰. This value of 21.7±0.2‰ for SRM 120c is now widely accepted as exemplified by the recent study published by Huang et al. (2018). It has also to be pointed out that an isotopic ratio of 21.7±0.16‰ for SRM 120c was determined for the first time by using quantitative fluorination 25 years ago (Lécuyer et al., 1993). Nevertheless, it must be underlined that the Florida phosphorite SRM 120c is a compositional, not an isotopic international reference, hence its oxygen isotope ratio has never been officially certified. In order to comply with the IUPAC recommendations (Brandt et al., 2014), a two-point calibration can also be performed with NBS 127, which is a barium sulfate calibrated reference material for oxygen isotopes ($\delta^{18}O$ = 9.3‰ VSMOW), as we proceeded in some recent papers (e.g. Rey et al., 2018; Goedert et al., 2018). However, we underline that NBS 127 is a different matrix, *i.e.* a barium sulfate instead of a silver phosphate, a chemical difference that needs to be taken into account during calibration procedures even though the recently developed "purge-and-trap" technology was able to overcome this pitfall as shown by Fourel et al. (2011). Moreover, the stock of NBS 127 international reference hosted by the IAEA is now exhausted, thus seriously reducing the possibility of calibrating the oxygen isotope composition of solid matrices. Therefore, the need for alternative calibrated material is becoming critical.

Here, we propose a simple and cheap protocol to synthesize silver phosphate in a wide range (≈ 35‰) of oxygen isotope compositions based on thermodynamic properties of the phosphate-water system, more specifically the equilibrium isotopic fractionation factor and the kinetics and temperature of isotopic exchange according to the data published by Lécuyer et al. (1999b). Beyond the theoretical considerations, an "Excel calculation sheet" is provided as a

supplementary material. This calculation sheet allows the $\delta^{18}O$ of precipitated Ag_3PO_4 to be predicted by tuning various parameters such as the temperature of oxygen isotope exchange, the duration of the reaction and the isotopic compositions of reactants.

2. Theoretical background

2.1. First-order kinetics of isotopic exchange between dissolved phosphate and water

The most common pH-dependent speciation of phosphorus in aqueous solution of low ionic strength are (1) the dihydrogen phosphate ion ($H_2PO_4^-$), (2) the hydrogen phosphate ion (HPO_4^{2-}), and (3) the phosphate ion (PO_4^{3-}) according to the three following chemical equilibria at 25°C (Zeebe and Wolf-Gladrow, 2001; Figure 1):

$$- H_3PO_4 \Leftrightarrow H_2PO_4^- + H^+ \quad (pK_{A1} = 1.9) \tag{1}$$

$$- H_2PO_4^- \Leftrightarrow HPO_4^{2-} + H^+ \quad (pK_{A2} = 6.1) \tag{2}$$

$$- HPO_4^{2-} \Leftrightarrow PO_4^{3-} + H^+ \quad (pK_{A3} = 8.9) \tag{3}$$

For seawater (pH ≈ 7.6 to 8.4), the dominant species is HPO_4^{2-} while in the case of natural freshwater it is either $H_2PO_4^-$ or HPO_4^{2-}. Lécuyer et al. (1999b) performed kinetics and isotopic experiments at a pH close to 5 for which $H_2PO_4^-$ was almost the only species present in solution (Figure 1). During first-order kinetics of reaction, the rate of isotopic exchange can be quantified by considering *f* as follows,

$$f = 1 - exp(-kt) = \frac{\delta^{18}O(PO_4)_i - \delta^{18}O(PO_4)_t}{\delta^{18}O(PO_4)_i - \delta^{18}O(PO_4)_e} \quad (4)$$

which is the mole fraction of exchanged isotopes between the phosphate ions and water molecules, while k is the rate constant (s^{-1}) of the isotopic reaction:

$$k = A.exp\left(-\frac{E_a}{RT}\right) \quad (5)$$

with A being the Arrhenius pre-exponential factor, E_a the activation energy ($kJ.mol^{-1}$) of the isotopic reaction, R the universal gas constant, T the absolute temperature (K), t the time (s), $\delta^{18}O(PO_4)_i$ the oxygen isotope composition of the reactant at t = 0, $\delta^{18}O(PO_4)_t$ the oxygen isotope composition of $H_2PO_4^-$ at any time t during the course of the isotopic reaction, and $\delta^{18}O(PO_4)_e$ the oxygen isotope composition of $H_2PO_4^-$ at isotopic equilibrium with H_2O. Note that when t = 0; f = 0 and $\delta^{18}O(PO_4)_t = \delta^{18}O(PO_4)_i$ while when $t \rightarrow \infty$; $f \rightarrow 1$ and $\delta^{18}O(PO_4)_t = \delta^{18}O(PO_4)_e$.

2.2. Experimental determination of thermodynamic variables (k, E_a and α)

2.2.1. The rate constant k

Lécuyer et al. (1999b) performed a best fit of their data with the Arrhenius law and found a strong temperature dependence of the rate constant k:

$$\log (k) = 12.35 \pm 0.63 - 6.98 \pm 0.24(10^3 T^{-1}) \quad (6)$$

A convenient way to report graphically the rate of isotopic exchange against time is to rewrite equation (4) as follows:

$$ln(1 - f) = -kt \quad (7)$$

The absolute value of the slope of the straight line for a given temperature T is the rate constant k of the reaction. Equation (7) also allows the half-time ($t_{1/2}$) of the isotopic reaction to be determined by solving it for f = 0.5 as follows:

$$t = \frac{0.693}{k} \quad (8)$$

2.2.1. The activation energy E_a of the reaction

Due to the tetrahedral architecture and covalent bonds (P–O) of the phosphate ion, the activation energy E_a necessary to promote the oxygen isotope exchange between phosphate and water molecules is very high with a value of 133.6±4.6 $kJmol^{-1}$ at pH = 5 (Lécuyer et al., 1999b). The activation energy E_a is calculated from the slope of the straight line defined by equation (6) combined to equation (5).

2.2.2. The fractionation coefficient α between $H_2PO_4^-$ and H_2O

At thermodynamic equilibrium, and according to the Mass Action Law, we can write the following isotopic exchange equation:

$$H_2P^{16}O_4^- + H_2{}^{18}O \quad \leftrightarrow H_2P^{18}O_4^- + H_2{}^{16}O \qquad (9)$$

Rearranging the terms in equation (9), the equilibrium constant or isotopic fractionation factor called α, which is determined for a given temperature T, is expressed as follows:

$$\alpha_{(H_2PO_4^- - H_2O)} = \frac{\left[\frac{^{18}O}{^{16}O}\right]_{H_2PO_4^-}}{\left[\frac{^{18}O}{^{16}O}\right]_{H_2O}} \qquad (10)$$

It is worthy to note that this temperature-dependent fractionation factor α must be independent from the isotopic compositions of both reactants according to Northrop and Clayton (1966). Lécuyer et al. (1999b) determined experimentally $\alpha(H_2PO_4^- - H_2O)$ in the temperature range 75 to 135°C:

$$10^3 \ln\alpha_{(H_2PO_4^- - H_2O)} = 18.35 \pm 0.37 (10^3 T^{-1}) - 32.29 \pm 1.01 \qquad (11)$$

3. Application to the synthesis of silver phosphate of known oxygen isotope ratio

3.1. Experimental protocol of silver phosphate precipitation

We present a protocol of silver phosphate precipitation from a highly soluble salt in water (solubility = 25 g.100 mL^{-1} at 25°C; Lide, 2005) such as the potassium dihydrogen

phosphate KH_2PO_4 (Lécuyer et al., 1999b). An aliquot of 50 mg of pure high-grade (> 99.5 wt%) Sigma-Aldrich™ synthetic KH_2PO_4 is dissolved in 35 mL of deionized water of known oxygen isotope composition. The resulting aqueous solutions have a concentration of 1 $g.L^{-1}$ (10.6 $mmol.l^{-1}$) of phosphate ions with a pH of 5 at ambient temperature. It is important to note that the amount of oxygen in water is much higher than in the pool of dissolved phosphate (oxygen molar ratio between H_2O and $KH_2PO_4 \approx 5000$), consequently the change in the oxygen isotope composition before and after equilibrium is not detectable with respect to the analytical uncertainties (1σ = 0.05‰ for the $\delta^{18}O$ of H_2O). The solutions are transferred into Ace Glass™ pyrex tubes sealed with a threaded teflon plug. Each set of tubes for a given temperature is placed in a high precision oven for run-times defined by the user. Samples are withdrawn at desired times and quenched in cold water to room temperature within a few minutes. Each sample of dissolved phosphate is quantitatively precipitated as silver phosphate (chemical yields are close to 100%) according to the protocol determined by Firsching (1961), which means that all the dissolved phosphate species ($\approx H_2PO_4^-$), are converted into Ag_3PO_4. For a chemical yield of 100%, the expected amount of silver phosphate is close to 150 mg. Running an experiment batch with ten Ace Glass™ pyrex tubes at the same time ensures the production of about 1.5 g of silver phosphate crystals of predicted oxygen isotope composition.

3.2. Oxygen isotope analysis of silver phosphate

Oxygen isotope compositions are measured using a high-temperature pyrolysis technique involving a VarioPYROcube™ elemental analyzer (EA) interfaced in continuous flow (CF) mode to an Isoprime™ isotopic ratio mass spectrometer (IRMS) (EA-Py-CF-IRMS

245 technique (Lécuyer et al., 2007; Fourel et al., 2011) at the University Claude Bernard Lyon 1.
246 For each sample, 5 aliquots of 300 µg of Ag_3PO_4 are mixed with 300 µg of pure carbon black
247 powder and loaded in silver foil capsules. Pyrolysis is performed at a temperature of 1450°C.
248 Measurements are calibrated against the SRM 120c (natural Miocene phosphorite from Florida)
249 and the NBS 127 (barium sulfate, $BaSO_4$: $\delta^{18}O$ = 9.3‰ VSMOW). The $\delta^{18}O$ of SRM 120c is
250 fixed at 21.7‰ (VSMOW) according to Lécuyer et al. (1993) who determined this value by
251 fluorinating silver phosphate crystals (n = 25, 1σ = 0.16) at 600°C for 12 hours and calibrated
252 the oxygen isotope ratios with the calibrated reference material NBS 28 quartz (9.5±0.2‰), and
253 measurement standards that are the "Snowbird" quartz (16.1±0.1‰) and the tholeiitic basaltic
254 glass standard CIRCE 93 (5.6±0.1‰).
255
256 **3.3. Predicted oxygen isotope composition of synthesized silver phosphate**
257
258 According to equation (4), for any temperature T, k and $\delta^{18}O(PO_4)_e$ are calculated, t
259 and $\delta^{18}O(PO_4)_i$ are measured, which means that $\delta^{18}O(PO_4)_t$ can be predicted as follows:
260
261 $$\delta^{18}O(PO_4)_t = \delta^{18}O(PO_4)_i - \{\delta^{18}O(PO_4)_i - \delta^{18}O(PO_4)_e\}\{1 - \exp(-kt)\} \quad (12)$$
262
263 We emphasize that the recommended working range of temperature is from 110°C to
264 130°C. Indeed, below a temperature of 110°C, kinetics of reaction is so slow that significant
265 isotopic exchange takes months, or even years when temperature is below 100°C. Then, above
266 a temperature of 130°C, the Ace Glass™ pyrex tubes sealed with a threaded teflon plug could
267 start to leak, leading to a shift of the initial oxygen isotope ratio of water. Finally, we provide
268 an "Excel calculation sheet" (Supplementary File) that automatically computes the oxygen

isotope composition of the precipitated silver phosphate depending on time t and temperature T of isotopic exchange as well as the oxygen isotope compositions of reactants KH_2PO_4 and H_2O at t = 0. Predicted oxygen isotope compositions of synthesized silver phosphate range from -7 to +31‰ VSMOW for a temperature range comprised between 110°C and 130°C and a range of water $\delta^{18}O$ from -20 to +15‰ VSMOW (Figure 2). For example, we have provided a calculation table (Supplementary File) showing a possible tuning of the parameters described above to obtain silver phosphate crystals with a $\delta^{18}O$ value (‰ VSMOW) that mimics that certified for the NBS 127 barium sulfate international reference.

In order to further demonstrate the efficiency of this method, we analysed the oxygen isotope compositions of three silver phosphates with expected $\delta^{18}O$ values ranging from about +10 to +22 ‰ VSMOW (Table 1), which cover the most common range of documented $\delta^{18}O$ values for natural dissolved phosphate and apatites. We reported the measured $\delta^{18}O$ values as a function of the expected ones and we obtained a strong linear correlation with a slope close to 1 (a = 1.032±0.029) and an intercept close to 0 (b = -0.794±0.466) (Figure 3). Within this isotopic variation range of 12‰, the calculated standard error is 0.24‰, which is comparable to the error associated with the admitted $\delta^{18}O$ value of SRM 120c. Therefore, we show that this method is suitable to produce robust in-house made calibrated Ag_3PO_4 for the oxygen isotope analysis of phosphatic compounds.

3.4. Potential application to the sulfate-water system

290 Furthermore, a similar protocol may be applied to the sulfate-water system to produce
291 barium sulfate of known oxygen isotope composition. Indeed, the required thermodynamic
292 properties such as the rate constant k, the activation E_a and the T-dependent isotopic
293 fractionation factor α have been determined by Chiba and Sakai (1985). The oxygen isotope
294 measurement of sulfates, whatever their natural or anthropogenic origin, could be very useful
295 to trace the mechanisms of their formation. For instance, sulfates may form in the atmosphere
296 from the oxidation of sulfur dioxide by hydroxyl radicals, hydrogen peroxide or ozone. Sulfates
297 may also result from a high-temperature oxidation to produce sulfur trioxide during combustion
298 processes before being ultimately hydrated to form sulfuric acid. Various oxygen isotope
299 fractionations could be associated with those chemical reactions, requiring the production of
300 calibrated barium sulfate with different $\delta^{18}O_{VSMOW}$ values.

301

302 **4. Conclusions**

303

304 The protocol we developed in this study is based on the equilibrium isotopic
305 fractionation factor α, the kinetics k and temperature T of isotopic exchange in the dissolved
306 phosphate-water system. It offers the possibility to produce in a reasonable amount of time (a
307 few days or a couple of weeks) about 1.5 g (the equivalent of 1,000 measurements) of silver
308 phosphate of known oxygen isotope composition. Moreover, the tuning of some parameters
309 (time and temperature of isotopic exchange and the compositions of reactants) allows the
310 synthesis of silver phosphate within a large range (≈35‰) of oxygen isotope ratios that match
311 the documented natural variability for both phosphate-bearing minerals and dissolved
312 phosphate of organic or inorganic origin.

313

Acknowledgements – this study has been founded by CNRS and IUF (CL).

316

317 **References**

318

319 **Amiot R., Lécuyer C., Buffetaut E., Escarguel G., Fluteau F. and Martineau F. (2006)**
320 Oxygen isotopes from biogenic apatites suggest widespread endothermy in Cretaceous
321 dinosaurs. **Earth and Planetary Science Letters, 246**, 41–54.

322

323 **Amiot R., Lécuyer C., Buffetaut E., Fluteau F., Legendre S. and Martineau F. (2004)**
324 Latitudinal temperature gradient during the Cretaceous Upper Campanian–Middle
325 Maastrichtian: $\delta^{18}O$ record of continental vertebrates. **Earth and Planetary Science Letters,**
326 **226**, 255–272.

327

328 **Angert A., Weiner T., Mazeh S. and Sternberg M. (2012)**
329 Soil phosphate stable oxygen isotopes across rainfall and bedrock gradients. **Environmental**
330 **Science and technology, 46,** 2156–2162.

331

332 **Barrick R.E. and Showers W.J. (1994)**
333 Thermophysiology of *Tyrannosaurus rex*: evidence from oxygen isotopes. **Science, 265**, 222–
334 224.

335

336 **Bauke S.L., Sperber (von) C., Tamburini F., Gocke M.I., Honermeier B., Schweitzer K.,**
337 **Baumecker M., Don A., Sandhage-Hofmann A. and Amelung W. (2018)**
338 Subsoil phosphorus is affected by fertilization regime in long-term agricultural experimental
339 trials. **European Journal of Soil Science, 69**, 103–112.

340

Bernard A., Lécuyer C., Vincent P., Amiot R., Bardet N., Buffetaut E., Cuny G., Fourel F., Martineau F., Mazin J.-M., and Prieur A. (2010)

Regulation of body temperature by some Mesozoic marine reptiles. **Science, 328**, 1379–1382.

Brandt W., Coplen T.B., Vogl J., Rosner M. and Prohaska T. (2014)

Assessment of international reference materials for isotope-ratio analysis (IUPAC Technical Report). **Pure and Applied Chemistry, 86**, 425–467.

Chang S.J. and Blake R.E. (2015)

Precise calibration of equilibrium oxygen isotope fractionations between dissolved phosphate and water from 3 to 37 °C. **Geochimica et Cosmochimica Acta, 150**, 314–329.

Chenery C., Müldner G., Evans J., Eckardt H. and Lewis M. (2010)

Strontium and stable isotope evidence for diet and mobility in Roman Gloucester, UK. **Journal of Archaeological Science, 37**, 150–163.

Chiba H. and Sakai H. (1985)

Oxygen isotope exchange rate between dissolved sulfate and water at hydrothermal temperatures. **Geochimica et Cosmochimica Acta, 49**, 993–1000.

Crowson R.A., Showers W.J., Wright E.K. and Hoering T.C. (1991)

A method for preparation of phosphate samples for oxygen isotope analysis. **Analytical Chemistry, 63**, 2397-2400.

Davies C.L., Surridge B.W. and Gooddy D.C. (2014)

Phosphate oxygen isotopes within aquatic ecosystems: Global data synthesis and future research priorities. **Science of the Total Environment, 496**, 563–575.

Evans J.A., Chenery C.A. and Fitzpatrick A.P. (2006)

Bronze age childhood migration of individuals near Stonehenge, revealed by strontium and oxygen isotope tooth enamel analysis. **Archaeometry, 48**, 309–321.

Firsching F.H. (1961)

Precipitation of silver phosphate from homogeneous solution. **Analytical Chemistry, 33**, 873-874.

Fourel F., Martineau F., Lécuyer C., Kupka H.J., Lange L., Ojeimi C. and Seed M. (2011)

$^{18}O/^{16}O$ ratios measurements of inorganic and organic materials by EA–Pyrolysis–IRMS continuous flow techniques. **Rapid Communications in Mass Spectrometry, 25**, 2691–2696.

Fricke H.C. and Rogers R.R. (2000)

Multiple taxon–multiple locality approach to providing oxygen isotope evidence for warm-blooded theropod dinosaurs. **Geology, 28**, 799–802.

Fricke H.C. and O'Neil J.R. (1996)

Inter- and intra-tooth variation in the oxygen isotope composition of mammalian tooth enamel phosphate: implications for palaeoclimatological and palaeobiological research. **Palaeogeography, Palaeoclimatology, Palaeoecology, 126**, 91–99.

Goedert J., Amiot R., Cuny G., Fourel F., Arnaud Godet F., Hernandez J.-A., Pedreira-Segade U. and Lécuyer C. (2017)

Miocene (Burdigalian) seawater and air temperatures estimated from the geochemistry of vertebrate remains from the Aquitaine Basin, France. **Palaeogeography, Palaeoclimatology, Palaeoecology, 481**, 14–28.

Goedert J., Lécuyer C., Amiot R., Wang X.,Cui L., Cuny G., Douay G., Fourel F., Simon L., Steyer S. and Zhu M. (2018)

Euryhaline ecology of early tetrapods revealed by stable isotopes. **Nature, 558**, 68–72.

Granger S.J., Harris P., Peukert S., Guo R., Tamburini F., Blackwell M.S., Howden N.J.K. and McGrath S. (2017)

Phosphate stable oxygen isotope variability within a temperate agricultural soil. **Geoderma, 285**, 64–75.

Gruau G., Legeas M., Riou C., Gallacier E., Martineau F. and Hénin O. (2005)

The oxygen isotope composition of dissolved anthropogenic phosphates: a new tool for eutrophication research? **Water Research, 39**, 232–238.

Halas S., Skrzypek G., Meier-Augenstein W., Pelc A. and Kemp H.F. (2011)

Inter-laboratory calibration of new silver orthophosphate comparison materials for the stable oxygen isotope analysis of phosphates. **Rapid Communications in Mass Spectrometry, 25**, 579–584.

Huang C., Joachimski M.M. and Gong Y. (2018)

Did climate changes trigger the Late Devonian Kellwasser Crisis? Evidence from a high-resolution conodont $\delta^{18}O_{PO4}$ record from South China. **Earth and Planetary Science Letters, 495**, 174–184.

Joachimski M.M., Lai X., Shen S., Jiang H., Luo G., Chen B., Chen J. and Sun Y. (2012) Climate warming in the latest Permian and the Permian–Triassic mass extinction. **Geology, 40**, 195–198.

Kolodny Y., Luz B. and Navon O. (1983) Oxygen isotope variations in phosphate of biogenic apatites, I. Fish bone apatite – rechecking the rules of the game. **Earth and Planetary Science Letters, 64**, 398–404.

Kolodny Y. and Raab M. (1988) Oxygen isotopes in phosphatic fish remains from Israel; paleothermometry of tropical Cretaceous and Tertiary shelf waters, **Palaeogeography, Palaeoclimatology, Palaeoecology, 64**, 59–67.

Lécuyer C., Amiot R., Trotter J. and Touzeau A. (2013) Calibration of the phosphate $\delta^{18}O$ paleothermometer with the calcium carbonate-water oxygen isotope fractionation equations. **Chemical Geology, 347**, 217–226.

Lécuyer C., Fourel F., Martineau F., Amiot R., Bernard A., Daux V., Escarguel G. and Morrison J. (2007)

High–precision determination of $^{18}O/^{16}O$ ratios of silver phosphate by EA–pyrolysis–IRMS continuous flow technique. **Journal of Mass Spectrometry, 42**, 36–41.

Lécuyer C., Grandjean P., Mazin J.-M. and De Buffrénil V. (1999a)

Oxygen isotope compositions of reptile bones and teeth: a potential record of terrestrial and marine paleoenvironments, in: E. Hoch, A.K. Brantsen (Eds.), **Secondary Adaptation to Life in Water II, University of Copenhagen (Denmark), Geologisk Museum**, p. 33.

Lécuyer C., Grandjean P. and Sheppard S.M.F. (1999b)

Oxygen isotope exchange between dissolved phosphate and water at temperatures temperatures <135°C: inorganic versus biological fractionations. **Geochimica et Cosmochimica Acta, 63**, 855–862.

Lécuyer C., Grandjean P., Barrat J.-A., Nolvak J., Emig C.C., Paris F. and Robardet M., 1998.

$\delta^{18}O$ and REE contents of phosphatic brachiopods: a comparison between modern and lower Paleozoic populations. **Geochimica et Cosmochimica Acta, 62**, 2429–2436.

Lécuyer C., Grandjean P., O'Neil J.R., Cappetta H. and Martineau F. (1993)

Thermal excursions in the ocean at the Cretaceous-Tertiary boundary (northern Morocco): $\delta^{18}O$ record of phosphatic fish debris. **Palaeogeography Palaeoclimatology Palaeoecology, 105**, 235-243.

Liang Y. and Blake R.E. (2009)

462 Compound-and enzyme-specific phosphodiester hydrolysis mechanisms revealed by $\delta^{18}O$ of
463 dissolved inorganic phosphate: Implications for marine P cycling. **Geochimica et**
464 **Cosmochimica Acta, 73**, 3782–3794.
465
466 **Lide D.R. (2005)**
467 CRC Handbook of Chemistry and Physics 86th Edition 2005-2006. **CRC Press, Taylor &**
468 **Francis**, Boca Raton, FL 2005, p. 4–79.
469
470 **Lightfoot E. and O'Connell T.C. (2016)**
471 On the use of biomineral oxygen isotope data to identify human migrants in the archaeological
472 record: intra-sample variation, statistical methods and geographical considerations. **PLOS**
473 **ONE**, DOI:10.1371/journal.pone.0153850.
474
475 **Longinelli A., Bartelloni M. and Cortecci G. (1976)**
476 The isotopic cycle of oceanic phosphate, I. 1976. **Earth and Planetary Science Letters, 32**,
477 389–392.
478
479 **Markel D., Kolodny Y., Luz B. and Nishri A. (1994)**
480 Phosphorus cycling and phosphorus sources in Lake Kinneret: Tracing by oxygen isotopes in
481 phosphate. **Israelian Journal of Earth Sciences, 43**, 165–178.
482
483 **McLaughlin, K., Kendall C., Silva S.R., Young, M. and Paytan A. (2006).**
484 Phosphate oxygen isotope ratios as a tracer for sources and cycling of phosphate in North San
485 Francisco Bay, California. **Journal of Geophysical Research, 111**, G03003,
486 doi:10.1029/2005JG000079.

Northrop D.A. and Clayton R.N. (1966)

Oxygen isotope fractionations in systems containing dolomite. **Journal of Geology, 74**, 174–196.

O'Neil J.R., Roe L.J., Reinhard E. and Blake R.E. (1994)

A rapid and precise method of oxygen isotope analysis of biogenic phosphate. **Israelian Journal of Earth Sciences, 43**, 203–212.

Pellegrini M., John Pouncett J., Jay M., Pearson M.P. and Richards M.P. (2016)

Tooth enamel oxygen "isoscapes" show a high degree of human mobility in prehistoric Britain. **Scientific Reports, 6**, 34986; doi: 10.1038/srep34986.

Pistocchi C., Tamburini F., Gruau G., Ferhi A., Trevisan D. and Dorioz J.-M. (2017)

Tracing the sources and cycling of phosphorus in river sediments using oxygen isotopes: Methodological adaptations and first results from a case study in France. **Water Research, 111**, 346–356.

Rey K., Day M.O., Amiot R., Goedert J., Lécuyer C., Sealy J. and Rubidge B.S. (2018)

Stable isotope record implicates aridification in late Capitanian mass extinction. **Gondwana Research, 59**, 1–8.

Sun Y., Wiedenbeck M., Joachimski M.M., Beier C., Kemner F. and Weinzierl C. (2016)

Chemical and oxygen isotope composition of gem-quality apatites: Implications for oxygen isotope reference materials for secondary ion mass spectrometry (SIMS). **Chemical Geology,**

440, 164–178.

Tamburini F., Pfahler V., von Sperber C., Frossard E. and Bernasconi S.M. (2014)
Oxygen isotopes for unraveling phosphorus transformations in the soil–plant system: A review. **Soil Science Society of America Journal, 78**, 38–46.

Touzeau A., Blichert-Toft J., Amiot R., Fourel F., Martineau F., Cockitt J., Hall K., Flandrois J.-P. and Lécuyer C. (2013)
Egyptian mummies record increasing aridity in the Nile valley from 5,500 to 1,500 B.P. **Earth Planetary and Science Letters, 375**, 92–100.

Tütken T. and Vennemann T. (2009)
Stable isotope ecology of Miocene large mammals from Sandelzhausen, southern Germany. **Paläontologische Zeitschrift, 83**, 207–226.

Vennemann T.W., Fricke H.C., Blake R.E., O'Neil J.R. and Colman A. (2002)
Oxygen isotope analysis of phosphates: a comparison of techniques for analysis of Ag_3PO_4. **Chemical Geology, 185**, 321–336.

Vennemann T. W. (2012)
Further comparison of methods of oxygen isotope analysis of phosphates and standards use. **IsoPhos 2012 Annual Meeting**, 25–29 June, Asconda, Switzerland.

von Sperber C., Lewandowski H., Tamburini F., Bernasconi S.M., Amelung W. and Frossard E. (2017)

Kinetics of enzyme-catalysed oxygen isotope exchange between phosphate and water revealed by Raman spectroscopy. **Journal of Raman Spectroscopy, 48**, 368–373.

White C.D., Spence M.W., Stuart-Williams H.L.Q. and Schwarcz H.P. (1998) Oxygen isotopes and the identification of geographical origins: The Valley of Oaxaca versus the Valley of Mexico. **Journal of Archaeological Science, 25**, 643–655.

Zeebe R. E. and Wolf-Gladrow D. (2001) CO_2 in Seawater: Equilibrium, Kinetics, Isotopes. **Elsevier Oceanography Series**, 65, pp. 346, Amsterdam, 2001.

548

549 **Table captions:**

550

551 Table 1: Comparison between measured ($\delta^{18}O_{measured}$) and predicted ($\delta^{18}O_{predicted}$) oxygen

552 isotope compositions of silver phosphate samples. The $\delta^{18}O_{predicted}$ values have been calculated

553 by using equation (6) and (12) knowing the temperature T and duration t of isotope exchange

554 reaction along with the initial compositions of dissolved phosphate $\delta^{18}O(PO_4)_i$ and water

555 $\delta^{18}O(H_2O)_i$ reactants. The $\delta^{18}O_{measured}$ values have been obtained by using the analytical

556 protocol presented in sections 3.1 and 3.2.

557

558

559 **Figure captions:**

560

561 Figure 1: pH-dependent speciation of dissolved phosphate in aqueous solution according to
562 Zeebe and Wolf-Gladrow (2001).

563

564 Figure 2: Oxygen isotope composition of dissolved phosphate (or precipitated silver phosphate)
565 as a function of time t (in days) of isotopic exchange for a temperature T of 110°C and a $\delta^{18}O$
566 of water of +15‰ (blue curve) and for a temperature T of 130°C and a $\delta^{18}O$ of water of -20‰
567 (red curve). After no more than 1 month of isotopic exchange between dissolved phosphate and
568 water, the precipitated silver phosphate crystals reach the isotopic equilibrium with water and
569 have $\delta^{18}O$ values close to +31‰ VSMOW (blue curve) and -7‰ VSMOW (red curve),
570 respectively.

571 For instance, the $\delta^{18}O$ of $H_2O(i)$ of +15‰ VSMOW can be obtained by collecting 1 L
572 of residual water obtained by evaporation at ambient temperature (≈ 20°C) under a laminar flow
573 hood of 50 L of deionized water with an initial $\delta^{18}O$ of -10.5‰ of which the ultimate source is
574 the Rhône river. The $\delta^{18}O$ of $H_2O(i)$ of -20‰ VSMOW can be obtained in Lyon, France, by
575 collecting frozen atmospheric vapour trapped inside a freezer working at a temperature of -
576 80°C.

577

578 Figure 3: Linear regression between the oxygen isotope compositions of measured and
579 predicted $\delta^{18}O$ values of three samples of synthesized silver phosphate. A slope of 1.032±0.029
580 and an intercept of -0.794±0.466 with a R^2 of 0.999 indicate a good fit between these two

581 variables. The standard error of 0.24‰ measures the robustness of the isotopic composition of
582 the precipitated silver phosphate that can be used as in-house made calibrated material.
583

584

585 **Supplementary File:**

586

587 Table: “Excel calculation sheet” that computes the oxygen isotope composition of the
588 precipitated silver phosphate depending on time t and temperature T of isotopic exchange along
589 with the oxygen isotope compositions of reactants KH_2PO_4 and H_2O at t = 0. The provided
590 example provided shows a possible tuning of the parameters described above to obtain silver
591 phosphate crystals with a $\delta^{18}O$ value (‰ VSMOW) similar to that certified for the NBS 127
592 barium sulfate international reference.
593 Description of column assignment: C0-C1 = temperature T; C2-C3 = rate constant k; C4-C5 =
594 time t; C6 = fraction f of isotopic exchange; C7-C8 = oxygen isotope compositions of reactants
595 at t = 0; C9-C10 = isotopic fractionation factor α between dissolved phosphate and water; C11-
596 12 = oxygen isotope composition of dissolved phosphate at equilibrium at any time t.
597

Calibrated Material	$\delta^{18}O$(water) (‰ VSMOW)	Equilibration (days)	$\delta^{18}O(Ag_3PO_4)$ predicted (‰ VSMOW)	S.D.	$\delta^{18}O(Ag_3PO_4)$ measured (‰ VSMOW)	S.D.	N
CAL1	7.74	37	21.68	0.54	21.66	0.10	8
CAL3	-1.18	44	15.06	0.01	14.55	0.35	10
CAL2	-7.42	44	9.90	0.28	9.53	0.28	6

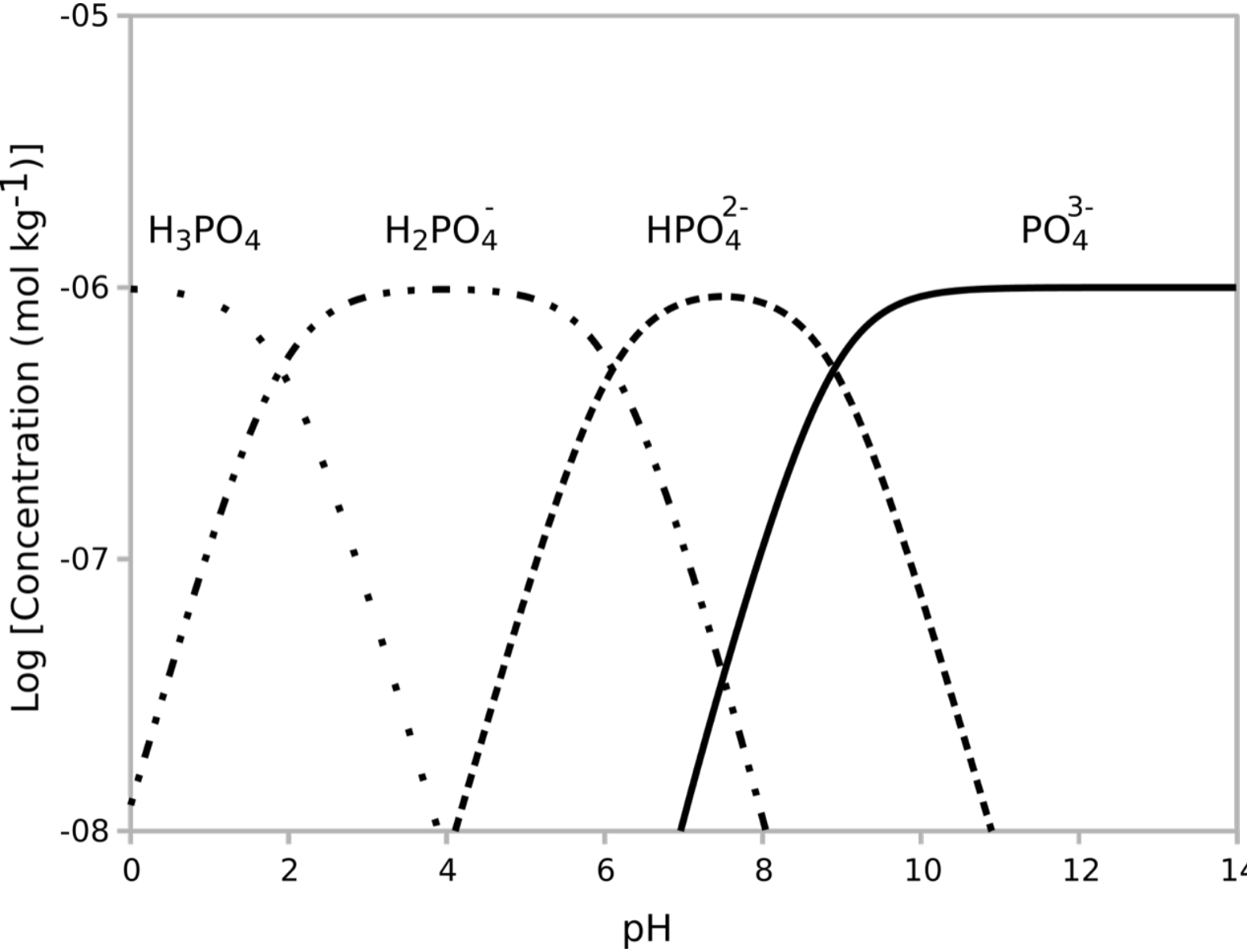
-05
-06
-07
-08
Log [Concentration (mol kg-1)]
H3PO4
H2PO4-
HPO4 2-
PO4 3-
0
2
4
6
8
10
12
14
pH

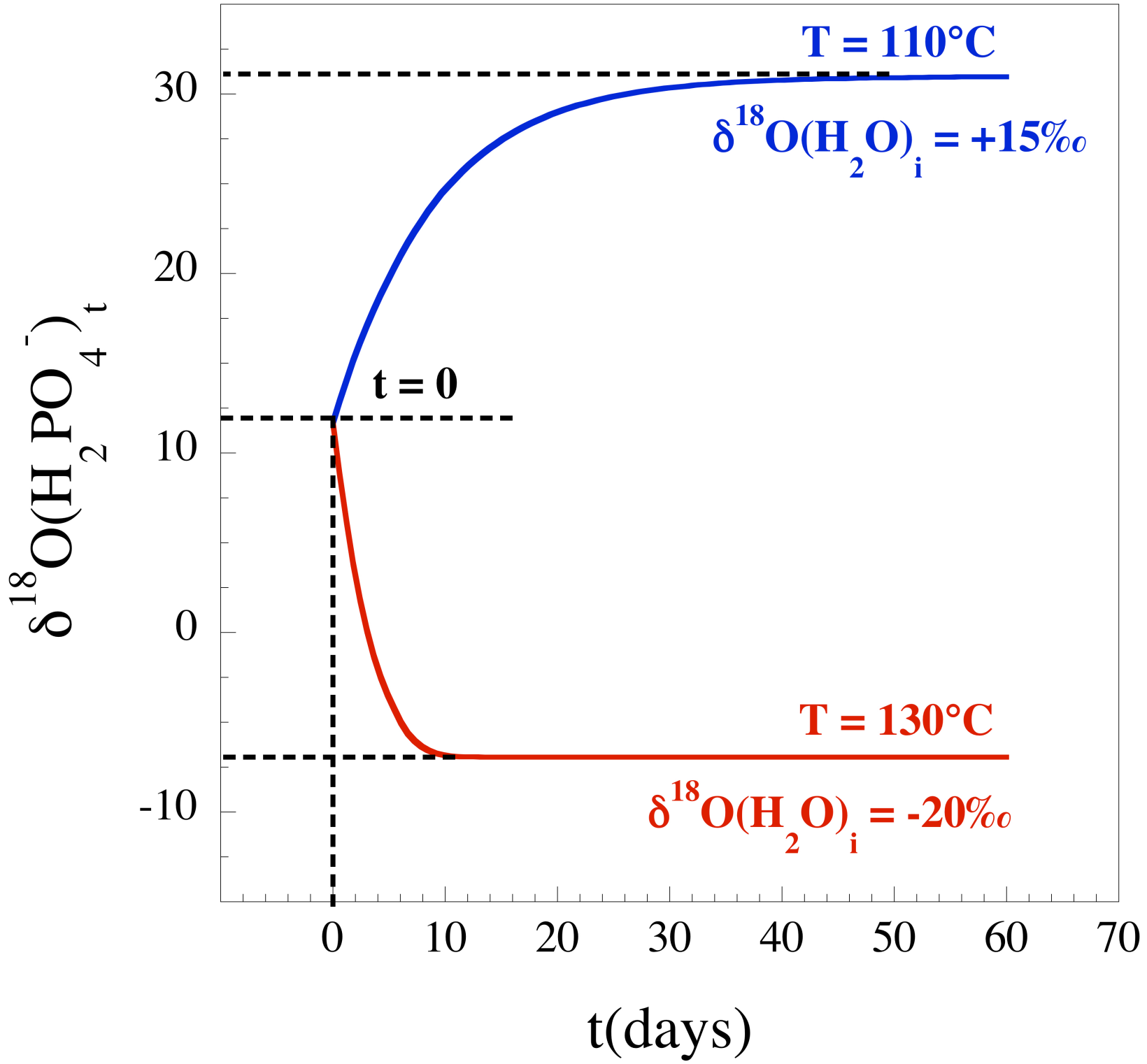
T = 110°C
δ18O(H2O)i = +15‰
t = 0
T = 130°C
δ18O(H2O)i = -20‰
δ18O(H2PO4-)t
t(days)
30
20
10
0
-10
0
10
20
30
40
50
60
70

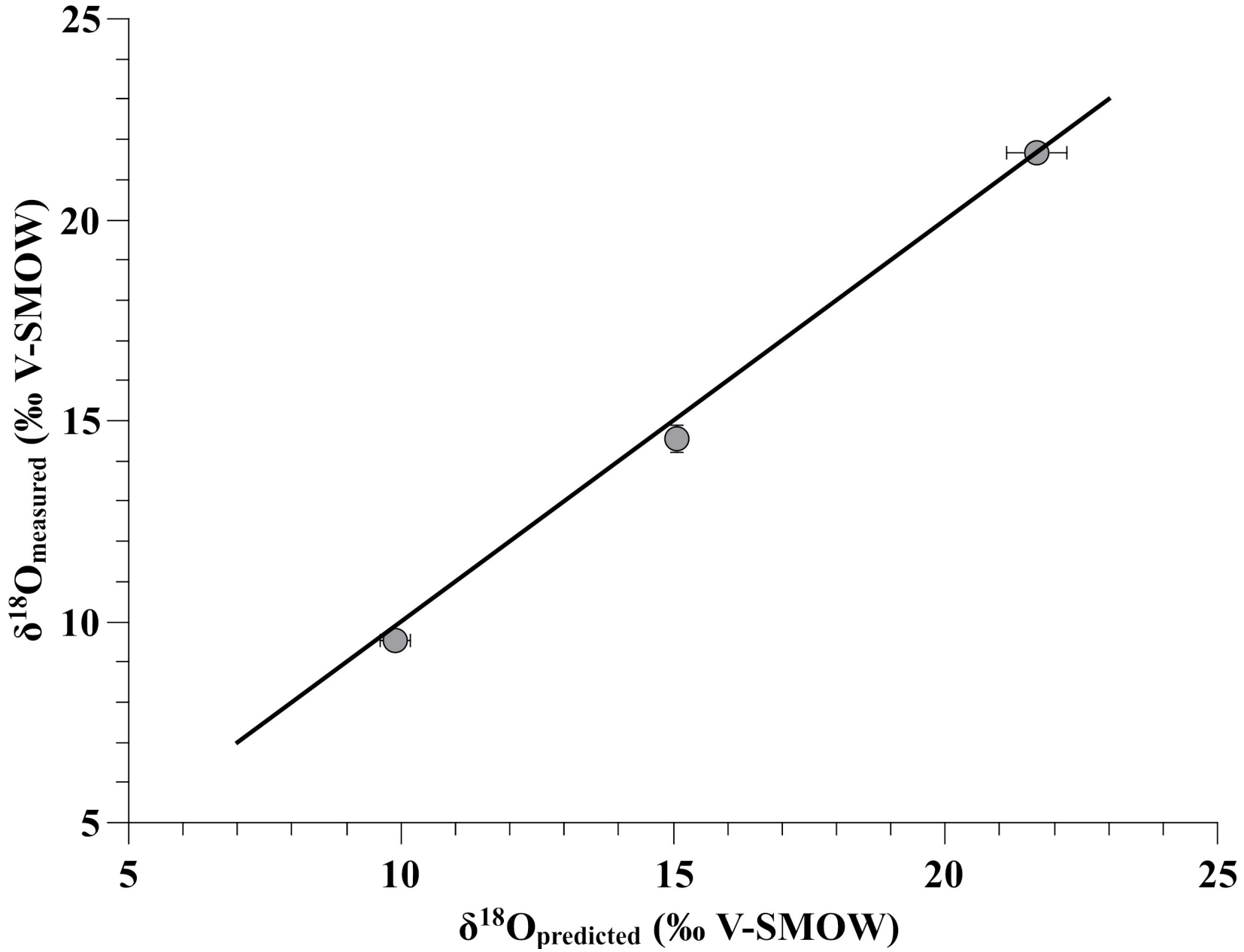
25
20
15
10
5
5
10
15
20
25
δ18Omeasured (‰ V-SMOW)
δ18Opredicted (‰ V-SMOW)